ARTICLE

ACS chemical biology

Functional and Structural Analysis of a Key Region of the Cell Wall Inhibitor Moenomycin

Shinichiro Fuse[†], Hirokazu Tsukamoto[†], Yanqiu Yuan[‡], Tsung-Shing Andrew Wang[†], Yi Zhang[†], Megan Bolla[†], Suzanne Walker[‡,*], Piotr Sliz[∥,§], and Daniel Kahne[∥,†,*]

[†]Department of Chemistry and Chemical Biology, Harvard University, Cambridge, Massachusetts 02138, [‡]Department of Microbiology and Molecular Genetics, [§]Department of Pediatrics, and [∥]Department of Biological Chemistry and Molecular Pharmacology, Harvard Medical School, Boston, Massachusetts 02115

ABSTRACT Moenomycin A (MmA) belongs to a family of natural products that inhibit peptidoglycan biosynthesis by binding to the peptidoglycan glycosyltransferases, the enzymes that make the glycan chains of peptidoglycan. MmA is remarkably potent, but its clinical utility has been hampered by poor physicochemical properties. Moenomycin contains three structurally distinct regions: a pentasaccharide, a phosphoglycerate, and a C25 isoprenyl (moenocinyl) lipid tail that gives the molecule its name. The phosphoglycerate moiety links the pentasaccharide to the moenocinyl chain. This moiety contains two negatively charged groups, a phosphoryl group and a carboxylate. Both the phosphoryl group and the carboxylate have previously been implicated in target binding but the role of the carboxylate has not been explored in detail. Here we report the synthesis of six MmA analogues designed to probe the importance of the phosphoglycerate. These analogues were evaluated for antibacterial and enzyme inhibitory activity; the specific contacts between the phosphoglycerate and the protein target were assessed by X-ray crystallography in conjunction with molecular modeling. Both the phosphoryl group and the carboxylate of the phosphoglycerate chain play roles in target binding. The negative charge of the carboxylate, and not its specific structure, appears to be the critical feature in binding since replacing it with a negatively charged acylsulfonamide group produces a more active compound than replacing it with the isosteric amide. Analysis of the ligand−protein contacts suggests that the carboxylate makes a critical contact with an invariant lysine in the active site. The reported work provides information and validated computational methods critical for the design of analogues based on moenomycin scaffolds.

Antibiotic-resistant bacterial infections pose a serious threat to public health, and there is an ongoing need for a pipeline of new antibacterial agents (*1, 2*). Compounds that have novel chemical structures or inhibit new targets in essential biosynthetic pathways are of particular interest because they are not expected to be susceptible to resistance mechanisms already established for other antibiotics. Moenomycin A (**1**, Figure 1, MmA) (*3*) is a natural product antibiotic that may serve as a promising lead for new antibiotics because it combines a novel structure with a unique mechanism of action. It inhibits peptidoglycan glycosyltransferases (PGTs), the enzymes that make the carbohydrate chains of bacterial peptidoglycan (PG) (*4*). Peptidoglycan biosynthesis is a major target for clinically used antibiotics, most of which are derived from natural products. Moenomycin is the only known natural product that directly inhibits the PGTs, and it provides a blueprint to guide the design of potent, broad-spectrum inhibitors to this family of antibiotic targets.

The biological activity of moenomycin is remarkable compared with that of most other natural product antibiotics: it is 10−1000 times more potent than vancomycin (*5, 6*) against Gram-positive organisms, with MICs below 0.1 μg mL^{-1}. It was developed for use as a growth promoter in animals, but its use in humans has been prevented by its poor physicochemical properties. Altering these properties has long been a goal. In a beautiful series of papers in the 1980s and 1990s, Welzel and co-workers used chemical synthesis to make a wide range of moenomycin analogues and elucidated several critical features of moenomycin that are essential for activity (*3*); however, a lack of detailed structural information on how moenomycin binds to its PGT targets eventually impeded progress in analogue design. In the

*Corresponding authors,
kahne@chemistry.harvard.edu,
suzanne_walker@hms.harvard.edu.

Received for review March 1, 2010
and accepted May 23, 2010.

Published online May 24, 2010

10.1021/cb100048q

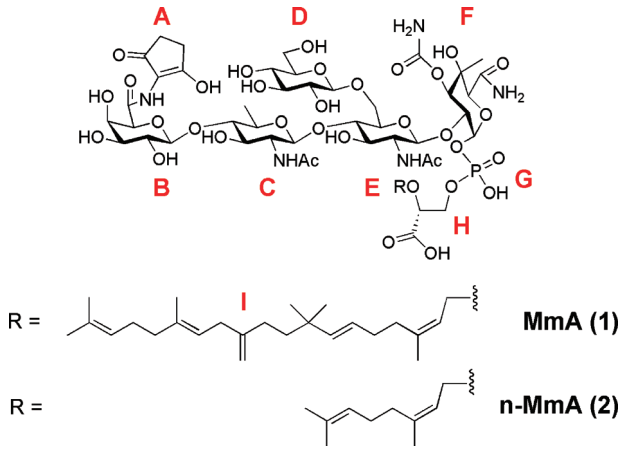

Figure 1. Chemical structures of MmA and n-MmA.

past 3 years, crystal structures of moenomycins bound to four different peptidoglycan glycosyltransferases have provided structural information to guide the design of new analogues. As is common, however, there are differences among the four complexes in the detailed contacts between the proteins and the ligands.

The most significant differences involve how the phosphoglycerate unit binds because these differences raise questions about the importance of the phosphoglycerate (*7–10*). We have used chemical synthesis combined with structural analysis to address its role, with particular emphasis on the carboxylate moiety. The importance of carboxylate of moenomycin in target binding has not been systematically explored previously, and there are notable differences among the crystal structures with respect to the protein contacts to this carboxylate. In one of the complexes, *Staphylococcus aureus* PBP2 (Figure 2, panel d), a conserved negatively charged glutamate side chain makes a proposed contact to the carboxylate, possibly *via* a bridging hydrogen bond (*9*). In another complex, *Escherichia coli* PBP1B, there are no side chains within 4 Å of the carboxylate (*8*). In the other two complexes, *Aquifex aeolicus* PBP1A and *S. aureus* MGT (Figure 2, panels b and e), an invariant lysine side chain is proposed to anchor the carboxylate (*7, 10*).

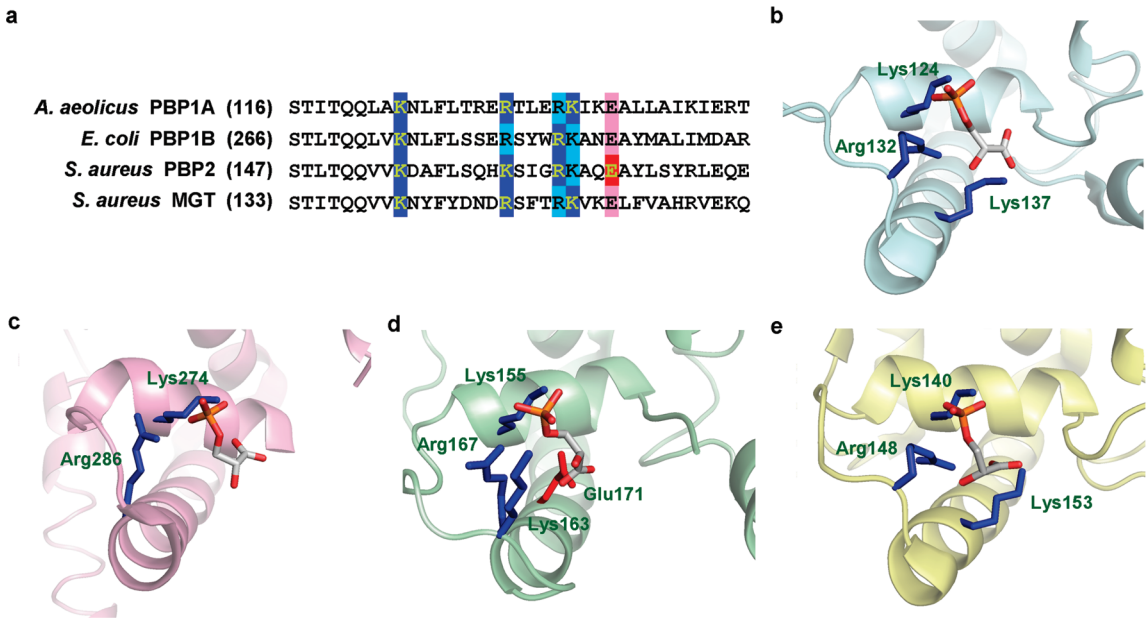

Figure 2. Sequence and structural alignment of charged residues. a) Charged residues in four PGTs that interact with MmA phosphoglycerate within 4 Å are highlighted in green letters as shown. These residues are highly conserved and well aligned, as shown in boxes, blue for positive and red for negative charged residues. Structural interactions of indicated residues and phosphoglycerate portion are drawn as stick models in b) *A. aeolicus* PBP1A (PDB code 3D3H), c) *E. coli* PBP1B (PDB code 3FWM), d) *S. aureus* PBP2 (PDB code 2OLV), and e) *S. aureus* MGT (PDB code 3HZS) crystal structures, shown as ribbon representations.

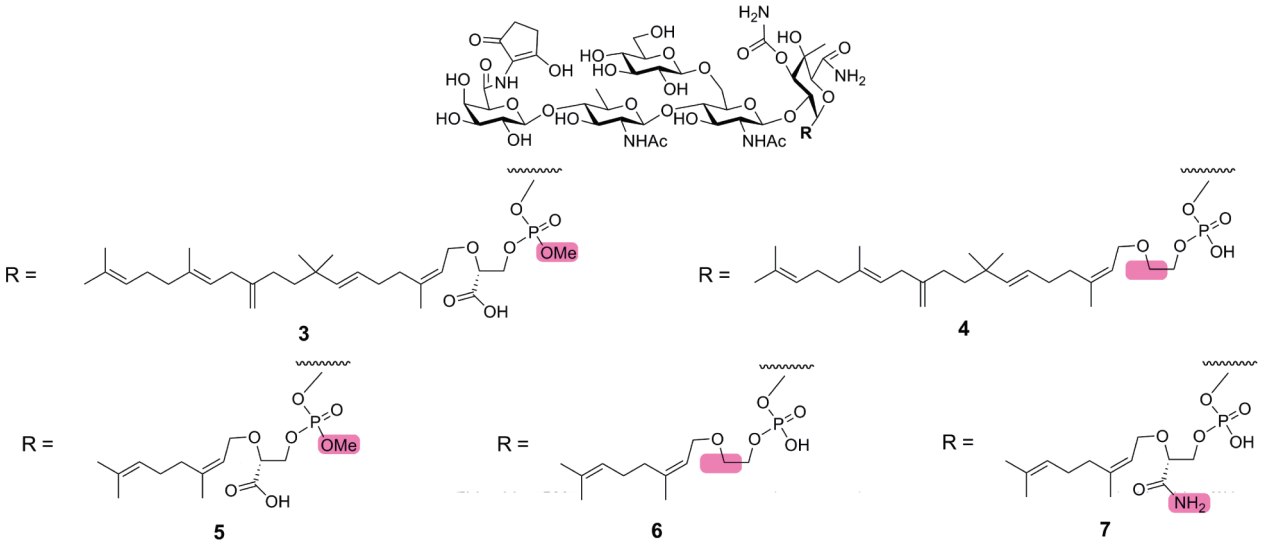

Figure 3. Chemical structures of MmA analogues.

The differences in the four PGT complexes raised questions about whether the carboxylate is critical for binding, and if so, whether the negative charge or the hydrogen bonding capability of the carboxyl group is more important. We have used a degradation-reconstruction approach to make six MmA analogues to address the role of the phosphoglycerate moiety of moenomycin in binding to peptidoglycan glycosyltransferases (*11*). We report here the multistep synthesis of these compounds, their biological evaluation, and modeling studies restrained by crystallographic data for co-complexes of two of the compounds. Our analysis indicates that the carboxylate plays a central role in binding to the target through energetically favorable ionic interactions with positively charged side chains in the active site. These interactions help orient the lipid chain for binding along the hydrophobic groove that funnels down from the active site to the membrane.

RESULTS AND DISCUSSION

Synthesis of MmA Analogues. In 2006 we reported the total synthesis of moenomycin as well as chemistry to degrade and reconstruct this natural product (*11, 12*). The latter chemistry allows us to independently change the phosphoryl group, the carboxylate, or the lipid of the phosphoglycerate moiety. Both these groups have previously been implicated in target binding (*13*), but the role of the carboxylate has not been explored in detail. Here we report the preparation of six derivatives of MmA in which individual features of the phosphoglycerate have been systematically varied. Two series of moenomycin compounds were prepared, one containing the natural C25 isoprenyl chain (**3** and **4**, Figure 3) and the other containing a neryl (C10) chain (**5** and **6**, Figure 3). In each series we synthesized one derivative in which the phosphoryl group was capped (**3** and **5**, Figure 3) and another in which the carboxylate was removed (**4** and **6**, Figure 3). In the C10 series, we also synthesized the isosteric carboxamide analogue **7** (Figure 3), which maintains the hydrogen-bonding network available to the carboxylate but removes the charge, and the acylsulfonamide analogue **34** (Scheme 3), which maintains the charge. The synthesis of each analogue required approximately 14 steps, and the combined syntheses of six different analogues highlights the utility of the synthetic methods we previously developed to degrade and reconstruct analogues of this densely functionalized natural product.

The desired phosphoglycerate derivatives were obtained by first preparing the appropriate lipid glycerates (Scheme 1). Briefly, alcohols **8** and **9** were prepared by coupling allyl bromides **11** (*11*) and **12** to the monotriisopropylsilyl protected ethylene glycol **13** followed by deprotection with TBAF. Alcohol **10** was prepared by amidation of carboxylic acid **16** (*11*), prepared from glycidol in six steps, followed by deprotection with DDQ. To obtain the desired phosphodiesters **22**–**25**, the C25-lipid-containing alcohol **8** and the C10-

Scheme 1. Synthesis of alcohols[a]

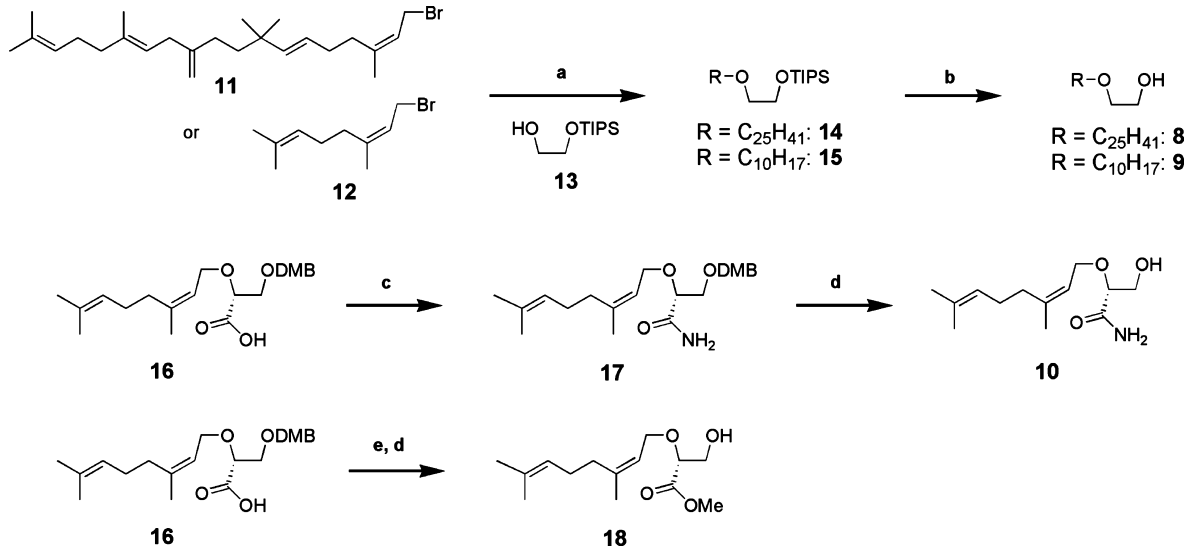

[a]Conditions: (a) NaH, THF/DMF (7:1), 0 °C; (b) TBAF, THF, 0 °C (**8**: 63% in 2 steps, **9**: 72% in 2 steps); (c) $ClCO_2Et$, Et_3N, *t*-BuOMe, RT, then NH_4OAc (70%); (d) DDQ, CH_2Cl_2/pH 7 buffer (10:1), RT (**10**: 81%, **18**: 72%); (e) $TMSCHN_2$, CH_2Cl_2/MeOH (1:1), −60 °C (quant).

lipid-containing alcohols **9**, **10**, and **18** were subjected to condensation with the core pentasaccharide *H*-phosphonate **21** (Scheme 2), which was prepared from MmA (**1**) (*11*). Competing esterification of alcohols **9** and **10** by 1-adamantanecarbonyl chloride (*14*) can be suppressed if addition of the 1-adamantanecarbonyl chloride is added as a solution in pyridine at 0 °C. Treatment with carbon tetrachloride (*15, 16*) effects *in situ* oxidation to form the corresponding phosphodiesters **22**−**25** selectively without affecting other chemically sensitive functionality (*e.g.*, the 2-amino-1,3-cyclopentadione of the A-ring and olefins within the isoprenoid chain). Subsequent saponification of the phosphodiesters **22**−**24** afforded the phosphoglycols **4** and **6** and the phosphoglyceramide **7** in satisfactory yield (Scheme 2 and Figure 3). Methyl phosphates **3** and **5** (Figure 3) were prepared by selective hydrolysis of methyl esters **19** and **26** under alkaline conditions (Scheme 2). Hydrolysis of the methyl phosphate was not observed under these reaction conditions.

The desired acylsulfonamide **34** (Scheme 3) was prepared by coupling the pentasaccharide lactol **20** with the protected acylsulfonamide **31.** Our route to the protected acylsulfonamide **31** is patterned on a synthetic route developed by Welzel (*17, 18*). The carboxylic acid **29** was prepared in two steps from known 1,3:4,6-di-*O*,*O*-(4-methoxybenzylidene)-D-mannitol (**27**) (*19*–*21*). Condensation of **29** with *N*-allyl-methanesulfonamide (*22*) was achieved under mild conditions using DCC in the presence of a stoichiometric amount of DMAP to afford optically pure *N*-allyl-protected acylsulfonamide **30**. An allyl group was chosen to protect the acylsulfonamide so that it could be selectively removed under neutral conditions (*e.g.*, palladium catalysis) (*23, 24*). Acid hydrolysis of the silyl ether **30** gave the primary alcohol **31**, which was used for coupling with the protected pentasaccharide **20**. The phosphoramidite was prepared *in situ* from **31**, coupled with lactol **20**, and further oxidized with *tert*-butylhydroperoxide to give phosphotriester **32**. The use of the phosphoramidite coupling (*25*–*28*) to prepare **32** turned out to be a more effective procedure than the *H*-phosphonate coupling method (*26, 29*) used to prepare compounds **2** and **4**-**7**. The phosphoramidite coupling method avoids transformation of lactol **20** to *H*-phosphonate **21** and the potential to competitively acylate **31**. To deprotect the acylsulfonamide **32**, a few allyl scavengers were tested (morpholine (*30*), *p*-toluenesulfinate (*31*), and barbituric acid (*32*)). Barbituric acid successfully removed the allyl group from **32** under palladium catalysis to give free acylsulfonamide **33**. These conditions for allyl group deprotection did not

SCHEME 2. Preparation of MmA analogues *2*−*7*[a]

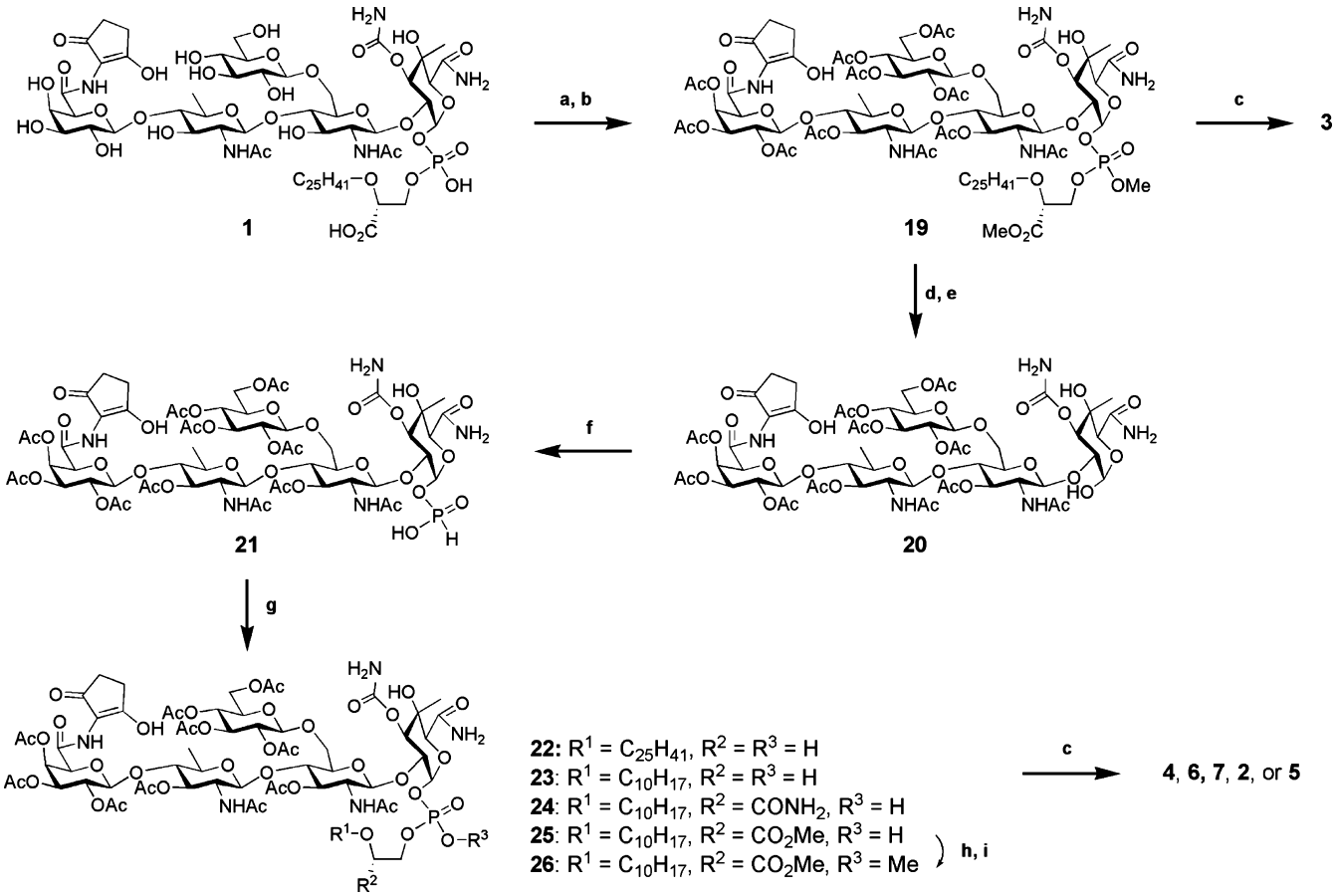

[a]Conditions: (a) Ac_2O, Py, RT; (b) $TMSCHN_2$, CH_2Cl_2/MeOH (1:1), −78 °C (61% in 2 steps); (c) 1 M LiOH aq or 1 M KOH aq, THF/H_2O (1:1), RT (**2**: 76%, **3**: 68%, **4**: quant, **5**: 77%, **6**: 97%, **7**: 66%); (d) TMSOTf, MS 4 Å, CH_2Cl_2, −78 to 0 °C; (e) saturated $NaHCO_3$ aq, RT, 1 h (73% in 2 steps); (f) 2-chloro-1,3,2-benzodioxaphosphorin-4-one, CH_3CN, −20 °C then H_2O (70%); (g) **8**, **9**, **10**, or **18**, 1-adamantanecarbonyl chloride, Py, MS 4 Å, RT, or 47 °C then CCl_4/NMM/CH_3CN/H_2O (2.4:1:1:1), RT (**22**: 55% based on 65% conversion, **23**: 88%, **24**: 68% based on 75% conversion, **25**: 63%); (h) **25**, Dowex 50WX8-100, MeOH, 0 °C; (i) $TMSCHN_2$, CH_2Cl_2/MeOH (1:1), −78 °C (61% in 2 steps).

decompose the chemically labile allylic ether of the isoprenoid chain (*33*). As far as we know, this is the first report of the use of an allyl group to protect an acylsulfonamide. The final global deprotection of **33** in mild base afforded the acylsulfonamide **34** (Scheme 3).

Evaluation of Biological Activity of MmA Analogues. We first evaluated the ability of the moenocinyl analogues **3** and **4** to inhibit the PGT activity of PBP2 from *S. aureus* (*34, 35*) and PBP2A from *E. faecalis* (*11*) using a previously described PGT assay (*36, 37*). The inhibitory ability of an analogue is reported as the half maximal inhibitory concentration (IC_{50}), the concentration at which the analogue inhibits 50% of the Lipid II polymerization activity catalyzed by PGTs. Polymerization activity was monitored by paper chromatography using a radiolabeled synthetic Lipid II substrate. We also determined the minimum inhibitory concentrations (MICs) of compounds **3** and **4** against laboratory strains of *S. aureus* and *E. faecalis* (Table 1). The MICs of analogues **3** and **4** were 5−10 and ~25 times higher, respectively, than that of MmA; however, the increased MICs were not reflected in the IC_{50} values for the analogues, which are similar to those for MmA (Table 1). One explanation for this observation is that the long moenocinyl chain interacts so strongly with the purified enzymes *via* nonspecific hydrophobic interactions that

SCHEME 3. Preparation of MmA acyl sulfonamide analogues 34[a]

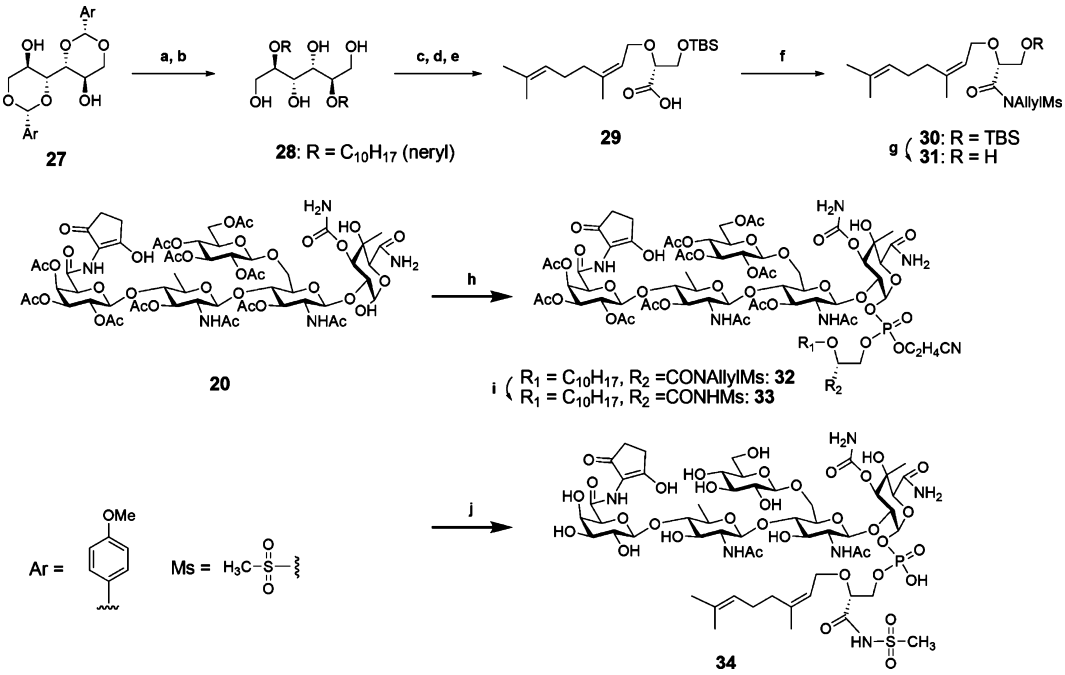

[a]Conditions: (a) NaH, **12**, DMF, RT; (b) AcOH/THF/H_2O (4:4:1), 50 °C (70% in 2 steps); (c) TBSCl, imidazole, cat. DMAP, CH_2Cl_2, RT; (d) $NaIO_4$, THF/H_2O (9:1), 50 °C; (e) $NaClO_2$, $NaH_2PO_4 \cdot H_2O$, 2-methyl-2-butene, *t*-BuOH/H_2O (5:1), RT (77% in 3 steps); (f) MsNHAllyl, DCC, DMAP, CH_2Cl_2, RT (57%); (g) AcOH/THF/H_2O (3:1:1), 50 °C (86%); (h) **31**, $ClP(OC_2H_4CN)N(i\text{-}Pr)_2$, DIEA, CH_3CN, then **20**, tetrazole, MS 3 Å, 0 °C−RT, then *t*-BuO_2H, 0−10 °C (33%); (i) barbituric acid, cat. $Pd(PPh_3)_4$, MeOH, RT; (j) 1 M LiOH·H_2O, THF/MeOH/H_2O (3:1:1) (46% in 2 steps).

the effects of changes elsewhere in the molecule are obscured. That is, the *in vitro* assay may be not capable of distinguishing activity differences among compounds with low nanomolar binding since the enzyme is stoichiometrically inhibited. We prepared the corresponding neryl analogues **5** and **6** to probe the importance of the phosphoryl group and carboxylate in the context of a molecule that does not bind to the target as tightly. We have previously shown that neryl analogue **2** (*11*), although it has no biological activity, has very good enzyme inhibitory activity (10-fold lower than that of the natural product in our assay); furthermore, it binds in the

TABLE 1. PGT inhibition and antibacterial activity for MmA and analogues

	IC_{50} (μM) [a]		MIC (μg mL^{-1})	
	S. aureus PBP2	*E. faecalis* PBP2A	*S. aureus* ATCC 29213	*E. faecalis* ATCC 29212
1	0.022 ± 0.001	0.035 ± 0.007	0.13	0.063
2	0.340 ± 0.209	0.203 ± 0.101	>250	>250
3	0.046 ± 0.039	0.059 ± 0.010	0.60	0.60
4	0.008 ± 0.001	0.011 ± 0.005	3.1	1.6
5	15 ± 4	23 ± 7	>250	>250
6	56 ± 14	57 ± 14	>250	>250
7	68 ± 26	88 ± 40	>250	>250

[a]The IC_{50} measurements were carried out under identical enzyme concentrations (30 nM for *S. aureus* PBP2; 40 nM for *E. faecalis* PBP2A).

same region of the active site as MmA itself and establishes similar contacts. Therefore, it is a good model system for assessing the importance of particular protein−ligand contacts. The IC_{50} values of analogues **5** and **6** were 2 orders of magnitude higher than that of **2**, showing that both the phosphoryl group and the carboxylate make critical contacts to the target (*7*). The magnitude of the change in binding for **5** and **6** are in the range that might be expected for an electrostatic contact between a ligand and a protein (*38, 39*). In all four reported moenomycin:PGT structures, the phosphoryl group makes a similar network of contacts to charged residues. These contacts likely explain the diminished affinity of **5** compared with **2**, as reflected in the IC_{50} values. However, the contacts to the carboxylate in the reported crystal structures vary (see the introduction). Therefore, although the lack of activity of the descarboxyl analogue highlights the importance of the carboxylate, we had to carry out further experiments to determine the structural basis for requiring this functional group.

To determine whether the hydrogen bonding network or the negative charge is most important for binding, we prepared carboxamide **7**, an uncharged isostere of **2** that is capable of hydrogen binding, and the acylsulfonamide analogue **34**. Acylsulfonamides are known to be fully deprotonated at physiological pH ($pK_a \sim 4-5$) (*40*) and are often used to mimic carboxylate groups. Although the acylsulfonamide is sterically larger than the carboxylate functionality, analysis of the X-ray structures of the complexes suggested there might be sufficient room for this group. Compound **7** was found to have an IC_{50} value comparable to that of the descarboxyl analogue against both PGTs tested; the IC_{50} of the acylsulfonamide analogue **34** was 5−10 fold better than that of the carboxamide isostere **7**. These results are consistent with the hypothesis that a negative charge in this region of MmA plays a key role in binding. The increased steric hindrance of the sulfonamide group may explain the observation that **34** is not as potent an inhibitor as **2**. Nevertheless, the activity of the analogue demonstrates that it is possible to make significant changes to this portion of the molecule provided the negative charge is maintained.

Computational Analysis of n-MmA Analogues Complexed with the aaPGT Domain. We attempted to obtain X-ray structural data on **5** and **6** complexed to aaPGT domain but were only partially successful. Although data sets were acquired for complexes with both ligands, the fractional occupancy was low. The positions of the phosphoryl groups were clear, but the density of the other parts was not as good. Therefore, we used molecular modeling to help rationalize the effects of the structural changes on binding for the analogues in Figure 3. Docking computations of moenomycin analogues were performed with LigPrep and Glide from the Schrödinger Suite using the X-ray structure of the PGT domain of *A. aeolicus* PBP1A (*aa*PGT) from the n-MmA co-complex (PDB code 3D3H) (*7*–*10*). Since moenomycin is much larger than a typical molecule used in docking (1200 *vs* 350 Da) and has more rotatable bonds than can be currently handled by the Schrödinger Suite, we used CEF trisaccharide fragments rather than the full pentasaccharide for docking (Figure 4, panels b, d, and f) (for sugar notation, see Figure 1). To validate the computational methods, we first confirmed that the docking results for the n-MmA CEF trisaccharide fragment were consistent with the crystal structure. The rmsd between the docked ligand and the ligand in the crystal structure of the complex was 1.1 Å, a very good agreement considering the large size of the docked ligand and the number of rotatable bonds. The docking computations were then extended to the CEF trisaccharide fragments of compounds **5** and **6** (Figure 4, panel d and f). Both docked in the same location as **2**. We used the Glide 4.0 XP scoring function to estimate protein−ligand binding affinities. This function incorporates unique water desolvation energy terms, hydrophobic enclosure, neutral−neutral single or correlated hydrogen bonds, and five categories of charged−charged hydrogen bonds (*41*). The Glide scores for the trisaccharide fragments of **2**, **5**,and **6** were −12, −10.6, and −9.2, respectively, an order consistent with the relative affinities of the compounds based on the IC_{50} measurements (*42*). The RMSDs between n-MmA in the crystal structure and the docked trisaccharide analogues of **5** and **6** were 1.3 and 2.7 Å, respectively.

We redocked the CEF trisaccharide frgments of compounds **5** and **6** using restraints obtained from the X-ray data for the parent compounds (**5** and **6**; see Methods). Although the occupancy in the X-ray structures of the complexes is low, strong electron density corresponding to the phosphate atoms is clearly visible and can be used as experimental constraints. A glide score of −11.2 was obtained for the CEF trisaccharide fragment of compound **5** in the restrained docking compu-

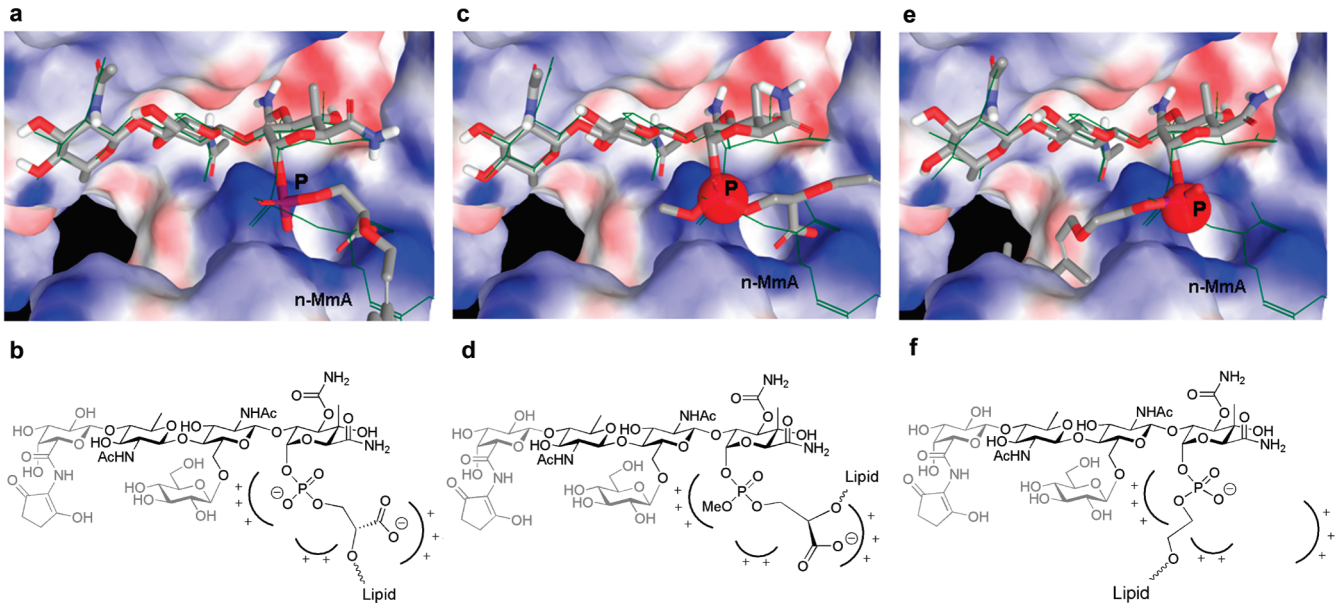

Figure 4. Structure-based docking results using CEF trisaccharide fragments of compounds 2, 5, and 6. Top panels represent close-up views of the ligand (shown in sticks with the phosphorus atoms labeled as P) docked in the active site of the *aa*PGT domain and overlaid on n-MmA (shown as green lines) from the crystal structure of the n-MmA:*aa*PGT co-complex. The protein receptor is shown as a surface presentation colored in red (oxygen), blue (nitrogen), and white (carbon). Bottom panels are chemical structures of the docked ligands. Figures in the top panels are made in Maestro. a) Docking of analogue 2 with *aa*PGT with no restraints. b) Chemical structure of compound 2 showing the CEF trisaccharide fragment used in the docking computations shown in black, with the rest shaded. c) Docking of analogue 5 with *aa*PGT using restraints for the phosphorus atom (the restraint is shown as a red ball). d) Chemical structure of compound 5 with the CEF trisaccharide fragment used in the docking computations shown in black, with the rest shaded. e) Docking of analogue 6 with *aa*PGT using restraints for the phosphorus atom. f) Chemical structure of compound 6 with the CEF trisaccharide fragment used in the docking computations shown in black, with the rest shaded.

tations; the rmsd compared to n-MmA was 1.4 Å, similar to the rmsd from unrestrained docking computations. A score of −9.6 and an rmsd of 2.6 Å were obtained for the CEF trisaccharide fragment of compound **6**, which is also similar to the rmsd from the unrestrained docking computations. It is notable that the neryl side chains in the docked structures of **2**, **5**, and **6** are oriented differently, suggesting that having the correctly positioned phosphoglycerate moiety also helps orient the lipid chain.

On the basis of the restrained docking computations, the high resolution X-ray structure of **2** complexed to the *A. aeolicus* PGT, and the IC_{50} values of the analogues we have synthesized, we propose that the carboxylate of moenomycin plays an important role in binding through a favorable electrostatic interaction with an invariant lysine in the active site. This contact is observed in two of the four reported moenomycin:PGT complexes (see Figure 2, panels b and e) (*7–10*). There may be a number of explanations for its absence in the other two complexes (*7–10*), including differences in crystallization conditions and the possibility that nonspecific hydrophobic interactions with the moenocinyl chain lead to misalignment of other functional groups. In any event, the relative activities of the descarboxyl analogues **4** and **6**, the carboxamide **7**, and the acylsulfonamide analogue **34** compared to those of the parent compounds clearly implicate the carboxylate negative charge in target binding.

Potential of Moenomycin As a Starting Point for Design of Clinically Useful Antibiotics. The PGTs are unexploited targets in the pathway for peptidoglycan biosynthesis. They are considered promising antibacterial targets because their structures are conserved, their functions are essential, they have no eukaryotic counterparts, and they are located on the external surface of the cytoplasmic membrane where they are accessible to molecules that cannot penetrate into the cell. The moenomy-

cins are the only blueprints to guide the design of analogues, and it is important to understand in detail how they bind. Although recent high resolution structures have provided detailed information on protein−ligand contacts, the importance of the contacts must be evaluated experimentally, particularly since there are some discrepancies. In this paper, we have focused on the role of the phosphoglycerate portion of moenomycin in binding to the PGT targets. Using a previously described method, we have been able to remove the phosphoglycerate lipid from the protected natural product and reattach a range of other phospholipids. We have prepared six different analogues of moenomycin containing changes to the phosphoglycerate-lipid portion of the molecule. On the basis of their enzyme inhibitory activity in conjunction with X-ray structural analysis and molecular docking, we have concluded that both the phosphoryl group and the carboxylate moiety of moenomycin form functionally important electrostatic interactions with conserved active site residues in the PGTs. The phosphate-protein contacts are similar in all four complexes and these contacts, shown in Figure 2, likely explain the importance of the phosphoryl group in anchoring moenomycin in the active site. In contrast, the carboxylate-protein contacts vary in the complexes, with two showing a salt bridge to an invariant lysine and the others showing no attractive interactions. Studies on our synthetic analogues support the importance of the observed salt bridge.

An interesting observation is that the relative importance of both the phosphoryl group and the carboxylate depends on the length of the lipid chain. No decrease in enzyme inhibitory activity was observed when either one of these groups was modified in the context of the C25 chain (compare **1** to **3** or **4**); in contrast, decreases of 2 to 3 orders of magnitude were observed when they were modified in the context of a C10 chain (compare **2** to **5**, **6**, **7**, or **34**). The results indicate that both the hydrophobic chain and the phosphoglycerate play a role in binding. One may contribute more to the energetics and the other may contribute more to the specificity. The C25 lipid clearly plays a major role in the biological activity of the natural product and probably contributes to target binding both by direct interactions with the hydrophobic funnel that leads to the membrane and by membrane anchoring. At the same time, it is also credited with the poor pharmacokinetic properties and high serum binding of moenomycin, so reducing its size is desirable. Although the C10 analogues are too short to retain biological activity, the C25 chain is longer than required for activity (*43*). An optimal lipid length has not yet been identified, but one implication of the work reported here is that any reduction in the size of the lipid chain increases the importance of maintaining appropriate polar active site contacts.

METHODS

Materials. Radiolabeled heptaprenyl-Lipid II was synthesized as described by Ye *et al.* (*36*). Moenomycin A (**1**) was extracted and purified from the feed stock flavomycin and purified as described (*11*). n-MmA (**2**) was synthesized as previously described (*11*). The synthesis and characterization of compounds **3**−**7** and **34** are described in Supporting Information. All other reagents and buffer components were purchased from Sigma-Aldrich.

Biological Activity Evaluation. IC_{50}'s against PBP2 from *S. aureus* and PBP2A from *E. faecalis* were obtained using a previously described assay (*36, 37*). PBP2 from *S. aureus* and PBP2A from *E. faecalis* were prepared as described in refs 11, 34, and 35. MIC values ($\mu g\ mL^{-1}$) against laboratory strains of *S. aureus* and *E. faecalis* were obtained using the standard broth microdilution assay (*44*). The MIC is defined as the lowest antibiotic concentration that resulted in no visible growth after incubation at 37 °C for 22 h.

Crystallization and Structural Determination. Crystals of protein *aa*PGT (PBP1A[51−243]) were obtained as described previously (*45*). Compounds **5** and **6** were soaked into PGT crystals at a concentration of 1 and 5 mM, respectively, in a stabilizing solution containing 100 mM HEPES, pH 7.5, 15% poly(ethylene glycol) 6000 (w/v) for 10 h. The crystals then were cryoprotected with 25% glycerol (v/v) and flash frozen in liquid nitrogen.

Data sets for two co-complexes were collected at NE-CAT beamline ID-24-C of the Advanced Photon Source (Argonne National Laboratories, Chicago). Data were indexed, integrated, and scaled with HKL2000 (*46*), and the data collection statistics are shown in Supplementary Table S1. The unit cell parameters for both co-complexes were very similar to the apo-*aa*PGT crystals, and therefore we placed the *aa*PGT coordinates (PDB code 2OQO) in the unit cell and refined the initial position by a rigid body protocol in CNS 1.225 (*47*). The protein model in each complex was then further improved by several iterative rounds of manual fitting in COOT 0.326 (*48*) and cycles of simulated annealing and temperature factor refinement in CNS. Inspection of final $2f_o - f_c$ and $f_o - f_c$ electron density maps confirmed the presence of ligand and the position of the phosphorus atoms. Detailed statistics pertaining to the final model are given in Supplementary Table S1.

Structure-Based Docking. Protein structure-based docking was performed with the Schrödinger Suite (www.schrodinger.com). The coordinates of a complex of the peptidoglycan glycosyltransferase domain from *A. aeolicus* and n-MmA (PDB code 3D3H) were first optimized using Protein Preparation Wizard. As part of this step we added hydrogen atoms, stripped water mol-

ecules, and performed energy minimization. The prepared coordinates were then used to calculate three grids, all centered at $x = 34.2$ Å, $y = 34.2$ Å, and $z = 10.3$ Å. The first grid did not incorporate any restraints and was subsequently used for docking the CEF trisaccharide fragments of n-MmA. The other two grids were calculated to dock the CEF trisaccharide fragments of compounds **5** and **6**, respectively, and therefore included positional restraints that would force the phosphorus atoms of the moenomycin derivatives to overlap, within 1.2 Å, with the position of the phosphorus atoms in the herein described X-ray structures. All ligands were prepared by the Schrödinger Ligprep module, and structure-based docking was performed with Glide version 50111 in the extra precision (XP) mode. The root-mean-square deviation was calculated for atoms in rings E and F and the phosphoglycerate group.

Accession Codes: The coordinates and structure factors have been deposited in the Protein Data Bank with PDB ID code 3NB6 (compound **5**:aaPGT) and 3NB7 (compound **6**:aaPGT).

Acknowledgment: This work was supported by the National Institutes of Health (RO1 GM076710 and RO1 GM066174) and National Science Foundation (0639193).

Supporting Information Available: This material is available free of charge *via* the Internet at http://pubs.acs.org.

REFERENCES

1. Sixteenth annual meeting of the Society of Healthcare Epidemiology of America in Chicago, Illinois. Abstract 173, 2006. (http://www.medscape.com/viewarticle/528623).
2. Anstead, G. M., Quinones-Nazario, G., and Lewis, J. S., 2nd. (2007) Treatment of infections caused by resistant *Staphylococcus aureus*, *Methods Mol. Biol. 391*, 227–258.
3. Welzel, P. (2005) Syntheses around the transglycosylation step in peptidoglycan biosynthesis, *Chem. Rev. 105*, 4610–4660.
4. van Heijenoort, J. (2001) Formation of the glycan chains in the synthesis of bacterial peptidoglycan, *Glycobiology 11*, 25R–36R.
5. Ostash, B., and Walker, S. (2005) Bacterial transglycosylase inhibitors, *Curr. Opin. Chem. Biol. 9*, 459–466.
6. Goldman, R. C., and Gange, D. (2000) Inhibition of transglycosylation involved in bacterial peptidoglycan synthesis, *Curr. Med. Chem. 7*, 801–820.
7. Yuan, Y., Fuse, S., Ostash, B., Sliz, P., Kahne, D., and Walker, S. (2008) Structural analysis of the contacts anchoring moenomycin to peptidoglycan glycosyltransferases and implications for antibiotic design, *ACS Chem. Biol. 3*, 429–436.
8. Sung, M. T., Lai, Y. T., Huang, C. Y., Chou, L. Y., Shih, H. W., Cheng, W. C., Wong, C. H., and Ma, C. (2009) Crystal structure of the membrane-bound bifunctional transglycosylase PBP1b from *Escherichia coli*, *Proc. Natl. Acad. Sci. U.S.A. 106*, 8824–8829.
9. Lovering, A. L., de Castro, L. H., Lim, D., and Strynadka, N. C. J. (2007) Structural insight into the transglycosylation step of bacterial cell-wall biosynthesis, *Science 315*, 1402–1405.
10. Heaslet, H., Shaw, B., Mistry, A., and Miller, A. A. (2009) Characterization of the active site of *S. aureus* monofunctional glycosyltransferase (Mtg) by site-directed mutation and structural analysis of the protein complexed with moenomycin, *J. Struct. Biol. 167*, 129–135.
11. Adachi, M., Zhang, Y., Leimkuhler, C., Sun, B. Y., LaTour, J. V., and Kahne, D. E. (2006) Degradation and reconstruction of moenomycin A and derivatives: Dissecting the function of the isoprenoid chain, *J. Am. Chem. Soc. 128*, 14012–14013.
12. Taylor, J. G., Li, X., Oberthur, M., Zhu, W., and Kahne, D. E. (2006) The total synthesis of moenomycin A, *J. Am. Chem. Soc. 128*, 15084–15085.
13. Welzel, P., Wietfeld, B., Kunisch, F., Schubert, T., Hobert, K., Duddeck, H., Muller, D., Huber, G., Maggio, J. E., and Williams, D. H. (1983) Moenomycin A: Further structural studies and preparation of simple derivatives, *Tetrahedron 39*, 1583–1591.
14. Andrus, A., Efcavitch, J. W., McBride, L. J., and Giusti, B. (1988) Novel activating and capping reagents for improved hydrogen-phosphonate DNA synthesis, *Tetrahedron Lett. 29*, 861–864.
15. Mohe, N. U., Padiya, K. J., and Salunkhe, M. M. (2003) An efficient oxidizing reagent for the synthesis of mixed backbone oligonucleotides *via* the H-phosphonate approach, *Bioorg. Med. Chem. 11*, 1419–1431.
16. Sinha, N. D., and Cook, R. M. (1988) The preparation and application of functionalized synthetic oligonucleotides: III. Use of H-phosphonate derivatives of protected amino-hexanol and mercapto-propanol or mercapto-hexanol, *Nucleic Acids Res. 16*, 2659–2669.
17. Schubert, T., and Welzel, P. (1982) Optically-active glycerol derivatives from 1,3(*R*):4,6(*R*)-di-*O*-benzylidene-D-mannitol—the first structural analogs of moenomycin A, *Angew. Chem., Int. Ed. Engl. 21*, 137–138.
18. Schubert, T., Kunisch, F., and Welzel, P. (1983) 1,3(*R*):4,6(*R*)-Di-*O*-benzylidene-D-mannitol as a starting product for the synthesis of optically-active glycerol derivatives, *Tetrahedron 39*, 2211–2217.
19. Peters, U., Bankova, W., and Welzel, P. (1987) Platelet-activating-factor synthetic studies, *Tetrahedron 43*, 3803–3816.
20. Metten, K. H., and Welzel, P. (1990) Synthesis of the repeating unit of the capsular antigen of *Neisseria meningitidis* serogroup-H, *Tetrahedron 46*, 5145–5154.
21. Rampy, M. A., Pinchuk, A. N., Weichert, J. P., Skinner, R. W. S., Fisher, S. J., Wahl, R. L., Gross, M. D., and Counsell, R. E. (1995) Synthesis and biological evaluation of radioiodinated phospholipid ether stereoisomers, *J. Med. Chem. 38*, 3156–3162.
22. Whitehead, C. W., and Traverso, J. J. (1958) Diuretics. II. alkoxymercuration by mixed anion salts of mercury, *J. Am. Chem. Soc. 80*, 2182–2185.
23. Guibe, F. (1997) Allylic protecting groups and their use in a complete environment. Part I: Allylic protection of alcohols, *Tetrahedron 53*, 13509–13556.
24. Guibe, F. (1998) Allylic protecting groups and their use in a complex environment. Part II: Allylic protecting groups and their removal through catalytic palladium π-allyl methodology, *Tetrahedron 54*, 2967–3042.
25. Elie, C. J. J., Dreef, C. E., Verduyn, R., van der Marel, G. A., and van Boom, J. H. (1989) Synthesis of 1-*O*-(1,2-di-*O*-palmitoyl-*sn*-glycero-3-phosphoryl)-2-*O*-α-D-mannopyranosyl-D-myo-inositol: a fragment of mycobacterial phospholipids, *Tetrahedron 45*, 3477–3486.
26. Westerduin, P., Veeneman, G. H., Marugg, J. E., van der Marel, G. A., and van Boom, J. H. (1986) An approach to the synthesis of α-L-fucopyranosyl phosphoric monoesters and diesters *via* phosphite intermediates, *Tetrahedron Lett. 27*, 1211–1214.
27. Westerduin, P., Veeneman, G. H., and van Boom, J. H. (1987) Synthesis of diphosphorylated and diphosphonylated lipid a monosaccharide analogs *via* phosphite intermediates, *Recl. Trav. Chim. Pays-Bas 106*, 601–606.
28. Westerduin, P., Veeneman, G. H., van der Marel, G. A., and van Boom, J. H. (1986) Synthesis of the fragment GlcNAc-α(1→p→6)-GlcNAc of the cell-wall polymer of *Staphylococcus lactis* having repeating *N*-acetyl-D-glucosamine phosphate units, *Tetrahedron Lett. 27*, 6271–6274.
29. Hermans, J. P. G., Devroom, E., Elie, C. J. J., van der Marel, G. A., and van Boom, J. H. (1986) An approach to the preparation of glycosyl phosphates using salicylchlorophosphite as the phosphitylating reagent, *Recl. Trav. Chim. Pays-Bas 105*, 510–511.
30. Friedrich-Bochnitschek, S., Waldmann, H., and Kunz, H. (1989) Allyl esters as carboxy protecting groups in the synthesis of *O*-glycopeptides, *J. Org. Chem. 54*, 751–756.

31. Honda, M., Morita, H., and Nagakura, I. (1997) Deprotection of allyl groups with sulfinic acids and palladium catalyst, *J. Org. Chem. 62*, 8932–8936.
32. Kunz, H., and Marz, J. (1992) Synthesis of glycopeptides with Lewis[a] antigen side-chain and HIV peptide-T sequence using the trichloroethoxycarbonyl allyl ester protecting group combination, *Synlett* 591–593.
33. Tsukamoto, H., Suzuki, T., and Kondo, Y. (2007) Remarkable solvent effect on Pd(0)-catalyzed deprotection of allyl ethers using barbituric acid derivatives: Application to selective and successive removal of allyl, methallyl, and prenyl ethers, *Synlett* 3131–3136.
34. Barrett, D., Leimkuhler, C., Chen, L., Walker, D., Kahne, D., and Walker, S. (2005) Kinetic characterization of the glycosyltransferase module of *Staphylococcus aureus* PBP2, *J. Bacteriol. 187*, 2215–2217.
35. Leimkuhler, C., Chen, L., Barrett, D., Panzone, G., Sun, B., Falcone, B., Oberthur, M., Donadio, S., Walker, S., and Kahne, D. (2005) Differential inhibition of *Staphylococcus aureus* PBP2 by glycopeptide antibiotics, *J. Am. Chem. Soc. 127*, 3250–3251.
36. Ye, X. Y., Lo, M. C., Brunner, L., Walker, D., Kahne, D., and Walker, S. (2001) Better substrates for bacterial transglycosylases, *J. Am. Chem. Soc. 123*, 3155–3156.
37. Chen, L., Walker, D., Sun, B., Hu, Y., Walker, S., and Kahne, D. (2003) Vancomycin analogues active against vanA-resistant strains inhibit bacterial transglycosylase without binding substrate, *Proc. Natl. Acad. Sci. U.S.A. 100*, 5658–5663.
38. Fersht, A. R., Shi, J. P., Knill-Jones, J., Lowe, D. M., Wilkinson, A. J., Blow, D. M., Brick, P., Carter, P., Waye, M. M., and Winter, G. (1985) Hydrogen bonding and biological specificity analysed by protein engineering, *Nature 314*, 235–238.
39. Bartlett, P. A., and Marlowe, C. K. (1987) Evaluation of intrinsic binding energy from a hydrogen bonding group in an enzyme inhibitor, *Science 235*, 569–571.
40. King, J. F. (1991) Acidity, In *The Chemistry of Sulphonic Acids, Esters, and Their Derivatives* (Patai, S., Rappoport, Z., Eds.), pp 251–259, John Wiley & Sons, Ltd., New York.
41. Friesner, R. A., Murphy, R. B., Repasky, M. P., Frye, L. L., Greenwood, J. R., Halgren, T. A., Sanschagrin, P. C., and Mainz, D. T. (2006) Extra precision glide: docking and scoring incorporating a model of hydrophobic enclosure for protein-ligand complexes, *J. Med. Chem. 49*, 6177–6196.
42. The methyl phosphonate in compound **5** has a chiral center. We modeled both diastereomers and obtained Glide scores for each. The values for each diastereomer are similar (−11.18 and −9.94), and we simply took the average value. The methyl phosphonate in compound **5** has a chiral center. We modeled both diastereomers and obtained Glide scores for each. The values for each diastereomer are similar (−11.18 and −9.94), and we simply took the average value.
43. Ostash, B., Doud, E. H., Lin, C., Ostash, I., Perlstein, D. L., Fuse, S., Wolpert, M., Kahne, D., and Walker, S. (2009) Complete characterization of the seventeen step moenomycin biosynthetic pathway, *Biochemistry 48*, 8830–8841.
44. Amsterdam, D. (1996) Susceptibility testing of antimicrobials in liquid media, In *Antibiotics in Laboratory Medicine* (Loman, V. Ed.), pp 52–111, Williams and Wilkins, Philadelphia, PA.
45. Yuan, Y., Barrett, D., Zhang, Y., Kahne, D., Sliz, P., and Walker, S. (2007) Crystal structure of a peptidoglycan glycosyltransferase suggests a model for processive glycan chain synthesis, *Proc. Natl. Acad. Sci. U.S.A. 104*, 5348–5353.
46. Otwinowski, Z., Minor, W. (1997) In *Methods in Enzymology*, pp 307–326, Academic Press, New York.
47. Brunger, A. T., Adams, P. D., Clore, G. M., DeLano, W. L., Gros, P., Grosse-Kunstleve, R. W., Jiang, J. S., Kuszewski, J., Nilges, M., Pannu, N. S., Read, R. J., Rice, L. M., Simonson, T., and Warren, G. L. (1998) Crystallography & NMR system: A new software suite for macromolecular structure determination, *Acta Crystallogr. D: Biol. Crystallogr. 54*, 905–921.
48. Emsley, P., and Cowtan, K. (2004) Coot: model-building tools for molecular graphics, *Acta Crystallogr. D: Biol. Crystallogr. 60*, 2126–2132.